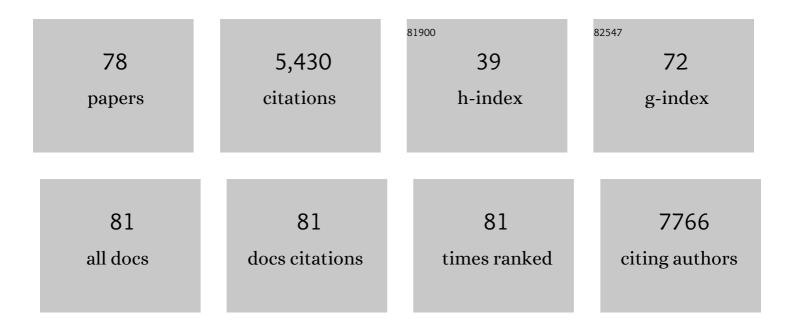
Robert S Weatherup

List of Publications by Year in descending order

Source: https://exaly.com/author-pdf/4307967/publications.pdf Version: 2024-02-01



#	Article	IF	CITATIONS
1	Carbon Nanotubes and Related Nanomaterials: Critical Advances and Challenges for Synthesis toward Mainstream Commercial Applications. ACS Nano, 2018, 12, 11756-11784.	14.6	388
2	In Situ Characterization of Alloy Catalysts for Low-Temperature Graphene Growth. Nano Letters, 2011, 11, 4154-4160.	9.1	258
3	Observing Graphene Grow: Catalyst–Graphene Interactions during Scalable Graphene Growth on Polycrystalline Copper. Nano Letters, 2013, 13, 4769-4778.	9.1	231
4	Understanding Fluoroethylene Carbonate and Vinylene Carbonate Based Electrolytes for Si Anodes in Lithium Ion Batteries with NMR Spectroscopy. Journal of the American Chemical Society, 2018, 140, 9854-9867.	13.7	219
5	In Situ Observations during Chemical Vapor Deposition of Hexagonal Boron Nitride on Polycrystalline Copper. Chemistry of Materials, 2014, 26, 6380-6392.	6.7	190
6	The Phase of Iron Catalyst Nanoparticles during Carbon Nanotube Growth. Chemistry of Materials, 2012, 24, 4633-4640.	6.7	180
7	<i>In Situ</i> Observations of the Atomistic Mechanisms of Ni Catalyzed Low Temperature Graphene Growth. ACS Nano, 2013, 7, 7901-7912.	14.6	163
8	Kinetic Control of Catalytic CVD for High-Quality Graphene at Low Temperatures. ACS Nano, 2012, 6, 9996-10003.	14.6	159
9	The Parameter Space of Graphene Chemical Vapor Deposition on Polycrystalline Cu. Journal of Physical Chemistry C, 2012, 116, 22492-22501.	3.1	155
10	Nucleation Control for Large, Single Crystalline Domains of Monolayer Hexagonal Boron Nitride via Si-Doped Fe Catalysts. Nano Letters, 2015, 15, 1867-1875.	9.1	139
11	Graphene-Passivated Nickel as an Oxidation-Resistant Electrode for Spintronics. ACS Nano, 2012, 6, 10930-10934.	14.6	138
12	Unraveling the Reaction Mechanisms of SiO Anodes for Li-Ion Batteries by Combining <i>in Situ</i> ⁷ Li and <i>ex Situ</i> ⁷ Li/ ²⁹ Si Solid-State NMR Spectroscopy. Journal of the American Chemical Society, 2019, 141, 7014-7027.	13.7	136
13	Photoelectron Spectroscopy at the Graphene–Liquid Interface Reveals the Electronic Structure of an Electrodeposited Cobalt/Graphene Electrocatalyst. Angewandte Chemie - International Edition, 2015, 54, 14554-14558.	13.8	135
14	Long-Term Passivation of Strongly Interacting Metals with Single-Layer Graphene. Journal of the American Chemical Society, 2015, 137, 14358-14366.	13.7	133
15	Magnetic tunnel junctions with monolayer hexagonal boron nitride tunnel barriers. Applied Physics Letters, 2016, 108, .	3.3	118
16	Controlling Catalyst Bulk Reservoir Effects for Monolayer Hexagonal Boron Nitride CVD. Nano Letters, 2016, 16, 1250-1261.	9.1	114
17	Towards a general growth model for graphene CVD on transition metal catalysts. Nanoscale, 2016, 8, 2149-2158.	5.6	114
18	Sub-nanometer Atomic Layer Deposition for Spintronics in Magnetic Tunnel Junctions Based on Graphene Spin-Filtering Membranes. ACS Nano, 2014, 8, 7890-7895.	14.6	109

#	Article	IF	CITATIONS
19	The influence of intercalated oxygen on the properties of graphene on polycrystalline Cu under various environmental conditions. Physical Chemistry Chemical Physics, 2014, 16, 25989-26003.	2.8	108
20	Time Evolution of the Wettability of Supported Graphene under Ambient Air Exposure. Journal of Physical Chemistry C, 2016, 120, 2215-2224.	3.1	108
21	Extrinsic Cation Selectivity of 2D Membranes. ACS Nano, 2017, 11, 1340-1346.	14.6	105
22	Introducing Carbon Diffusion Barriers for Uniform, High-Quality Graphene Growth from Solid Sources. Nano Letters, 2013, 13, 4624-4631.	9.1	104
23	CVD-Enabled Graphene Manufacture and Technology. Journal of Physical Chemistry Letters, 2015, 6, 2714-2721.	4.6	100
24	Interdependency of Subsurface Carbon Distribution and Graphene–Catalyst Interaction. Journal of the American Chemical Society, 2014, 136, 13698-13708.	13.7	95
25	Dissociative Carbon Dioxide Adsorption and Morphological Changes on Cu(100) and Cu(111) at Ambient Pressures. Journal of the American Chemical Society, 2016, 138, 8207-8211.	13.7	94
26	On the Mechanisms of Niâ€Catalysed Graphene Chemical Vapour Deposition. ChemPhysChem, 2012, 13, 2544-2549.	2.1	90
27	Graphene Membranes for Atmospheric Pressure Photoelectron Spectroscopy. Journal of Physical Chemistry Letters, 2016, 7, 1622-1627.	4.6	88
28	Insulator-to-Metallic Spin-Filtering in 2D-Magnetic Tunnel Junctions Based on Hexagonal Boron Nitride. ACS Nano, 2018, 12, 4712-4718.	14.6	88
29	Probing electrode/electrolyte interfaces in situ by X-ray spectroscopies: old methods, new tricks. Physical Chemistry Chemical Physics, 2015, 17, 30229-30239.	2.8	83
30	In Situ Observations of Phase Transitions in Metastable Nickel (Carbide)/Carbon Nanocomposites. Journal of Physical Chemistry C, 2016, 120, 22571-22584.	3.1	80
31	Substrate-assisted nucleation of ultra-thin dielectric layers on graphene by atomic layer deposition. Applied Physics Letters, 2012, 100, .	3.3	78
32	Stable, efficient p-type doping of graphene by nitric acid. RSC Advances, 2016, 6, 113185-113192.	3.6	66
33	Protecting nickel with graphene spin-filtering membranes: A single layer is enough. Applied Physics Letters, 2015, 107, .	3.3	65
34	In Situ Graphene Growth Dynamics on Polycrystalline Catalyst Foils. Nano Letters, 2016, 16, 6196-6206.	9.1	62
35	Graphene Liquid Enclosure for Single-Molecule Analysis of Membrane Proteins in Whole Cells Using Electron Microscopy. ACS Nano, 2017, 11, 11108-11117.	14.6	59
36	Measuring the proton selectivity of graphene membranes. Applied Physics Letters, 2015, 107, .	3.3	56

#	Article	IF	CITATIONS
37	Effects of polymethylmethacrylate-transfer residues on the growth of organic semiconductor molecules on chemical vapor deposited graphene. Applied Physics Letters, 2015, 106, .	3.3	54
38	Stability of graphene doping with MoO3 and I2. Applied Physics Letters, 2014, 105, .	3.3	49
39	Free-standing graphene membranes on glass nanopores for ionic current measurements. Applied Physics Letters, 2015, 106, .	3.3	45
40	Electrolyte Reactivity at the Charged Ni-Rich Cathode Interface and Degradation in Li-Ion Batteries. ACS Applied Materials & Interfaces, 2022, 14, 13206-13222.	8.0	45
41	Spin filtering by proximity effects at hybridized interfaces in spin-valves with 2D graphene barriers. Nature Communications, 2020, 11, 5670.	12.8	37
42	Formation of an Artificial Mg ²⁺ -Permeable Interphase on Mg Anodes Compatible with Ether and Carbonate Electrolytes. ACS Applied Materials & Interfaces, 2021, 13, 24565-24574.	8.0	36
43	A Peeling Approach for Integrated Manufacturing of Large Monolayer h-BN Crystals. ACS Nano, 2019, 13, 2114-2126.	14.6	35
44	In-situ study of growth of carbon nanotube forests on conductive CoSi2 support. Journal of Applied Physics, 2011, 109, .	2.5	33
45	Low temperature growth of carbon nanotubes on tetrahedral amorphous carbon using Fe–Cu catalyst. Carbon, 2015, 81, 639-649.	10.3	30
46	Environment-Dependent Radiation Damage in Atmospheric Pressure X-ray Spectroscopy. Journal of Physical Chemistry B, 2018, 122, 737-744.	2.6	30
47	Cycle-Induced Interfacial Degradation and Transition-Metal Cross-Over in LiNi _{0.8} Mn _{0.1} Co _{0.1} O ₂ –Graphite Cells. Chemistry of Materials, 2022, 34, 2034-2048.	6.7	28
48	2D Material Membranes for Operando Atmospheric Pressure Photoelectron Spectroscopy. Topics in Catalysis, 2018, 61, 2085-2102.	2.8	26
49	The origin of chemical inhomogeneity in garnet electrolytes and its impact on the electrochemical performance. Journal of Materials Chemistry A, 2020, 8, 14265-14276.	10.3	26
50	Hafnia nanoparticles – a model system for graphene growth on a dielectric. Physica Status Solidi - Rapid Research Letters, 2011, 5, 341-343.	2.4	25
51	Co-Catalytic Solid-State Reduction Applied to Carbon Nanotube Growth. Journal of Physical Chemistry C, 2012, 116, 1107-1113.	3.1	23
52	Structure of the Clean and Oxygen-Covered Cu(100) Surface at Room Temperature in the Presence of Methanol Vapor in the 10–200 mTorr Pressure Range. Journal of Physical Chemistry B, 2018, 122, 548-554.	2.6	23
53	Nitrogen controlled iron catalyst phase during carbon nanotube growth. Applied Physics Letters, 2014, 105, .	3.3	22
54	Carbon nanotube forest growth on NiTi shape memory alloy thin films for thermal actuation. Thin Solid Films, 2011, 519, 6126-6129.	1.8	19

#	Article	IF	CITATIONS
55	Crystal Orientation Dependent Oxidation Modes at the Buried Graphene–Cu Interface. Chemistry of Materials, 2020, 32, 7766-7776.	6.7	19
56	Atomic layer deposited oxide films as protective interface layers for integrated graphene transfer. Nanotechnology, 2017, 28, 485201.	2.6	18
57	Chemical vapour deposition of freestanding sub-60 nm graphene gyroids. Applied Physics Letters, 2017, 111, .	3.3	18
58	In situ and operando characterisation of Li metal – Solid electrolyte interfaces. Current Opinion in Solid State and Materials Science, 2022, 26, 100978.	11.5	18
59	The role of the sp2:sp3 substrate content in carbon supported nanotube growth. Carbon, 2014, 75, 327-334.	10.3	17
60	From Growth Surface to Device Interface: Preserving Metallic Fe under Monolayer Hexagonal Boron Nitride. ACS Applied Materials & Interfaces, 2017, 9, 29973-29981.	8.0	16
61	Reactive intercalation and oxidation at the buried graphene-germanium interface. APL Materials, 2019, 7, .	5.1	16
62	Co-catalytic Absorption Layers for Controlled Laser-Induced Chemical Vapor Deposition of Carbon Nanotubes. ACS Applied Materials & amp; Interfaces, 2014, 6, 4025-4032.	8.0	14
63	X-ray-Induced Fragmentation of Imidazolium-Based Ionic Liquids Studied by Soft X-ray Absorption Spectroscopy. Journal of Physical Chemistry Letters, 2018, 9, 785-790.	4.6	14
64	Oxidising and carburising catalyst conditioning for the controlled growth and transfer of large crystal monolayer hexagonal boron nitride. 2D Materials, 2020, 7, 024005.	4.4	13
65	Understanding metal organic chemical vapour deposition of monolayer WS ₂ : the enhancing role of Au substrate for simple organosulfur precursors. Nanoscale, 2020, 12, 22234-22244.	5.6	13
66	Low temperature growth of fully covered single-layer graphene using a CoCu catalyst. Nanoscale, 2017, 9, 14467-14475.	5.6	11
67	Gently does it!: <i>in situ</i> preparation of alkali metal–solid electrolyte interfaces for photoelectron spectroscopy. Faraday Discussions, 2022, 236, 267-287.	3.2	11
68	Compressive behavior and failure mechanisms of freestanding and composite 3D graphitic foams. Acta Materialia, 2018, 159, 187-196.	7.9	10
69	Identifying the catalyst chemical state and adsorbed species during methanol conversion on copper using ambient pressure X-ray spectroscopies. Physical Chemistry Chemical Physics, 2020, 22, 18806-18814.	2.8	9
70	Influence of Dissolved O ₂ in Organic Solvents on CuOEP Supramolecular Self-Assembly on Graphite. Langmuir, 2016, 32, 5526-5531.	3.5	7
71	Graphene-passivated nickel as an efficient hole-injecting electrode for large area organic semiconductor devices. Applied Physics Letters, 2020, 116, .	3.3	3
72	Electron Microscopy of Single Cells in Liquid for Stoichiometric Analysis of Transmembrane Proteins. Microscopy and Microanalysis, 2016, 22, 74-75.	0.4	2

#	Article	IF	CITATIONS
73	Observing Electrochemical Reactions on Suspended Graphene: An Operando Kelvin Probe Force Microscopy Approach. Advanced Materials Interfaces, 2021, 8, 2100662.	3.7	2
74	Enclosed Cells for Extending Soft X-ray Spectroscopies to Atmospheric Pressures and Above. ACS Symposium Series, 0, , 175-218.	0.5	2
75	Spatial variability in large area single and few-layer CVD graphene. , 2015, , .		1
76	Graphene Enclosure Facilitates Single-Molecule Analysis of ErbB2 Receptors in Intact, Hydrated Eukaryotic Cells by Electron Microscopy. Microscopy and Microanalysis, 2017, 23, 1304-1305.	0.4	0
77	Correlative Fluorescence and Electron Microscopy of Graphene-Enclosed Whole Cells for High Resolution Analysis of Cellular Proteins. Microscopy and Microanalysis, 2019, 25, 5-6.	0.4	0
78	Observing Formation of the Solid Electrolyte Interface By Operando Neutron Reflectivity. ECS Meeting Abstracts, 2020, MA2020-01, 528-528.	0.0	0